The XXII Symposium on Measuring Techniques in Turbomachinery
Transonic and Supersonic Flow in Cascades and Turbomachines
Lyon, France, 4 - 5 September 2014

TRANSIENT CONVECTION CALIBRATION OF HEAT TRANSFER GAUGES FOR HIGH ENTHALPY FLOWS

R.J. Lubbock, S. Luque, B.R. Rosic
Osney Thermo-Fluids Laboratory
Dept. of Engineering Science
University of Oxford

ABSTRACT

This paper presents a novel transient method for calibrating heat transfer gauges for convection measurements in high enthalpy flows. Previously only steady-state methods have been considered. These require cooling, which adds complexity and expense to the experimental design. The new method is simple, inexpensive, easy to adapt for different flow configurations and sensor geometries and quick to run across a wide range of conditions. The theory of the convection sensitivity of circular foil gauges is summarised as a basis for the design of the new calibration facility. The experimental design, method and data processing techniques are then presented along with some preliminary experimental results.

INTRODUCTION

There are few methods available for measuring wall heat flux in high enthalpy flows such as those present in gas turbine hot sections. Gardon Gauges, also known as Circular Foil Gauges, are most widely used owing to their high face-temperature capability, robustness, relatively small size and ease of installation. The main factors affecting the ability of these gauges to measure the *undisturbed* wall heat flux are the gauge sensitivity to convective heat transfer and the effects of the surface temperature discontinuity introduced by the gauge. The former is specific to circular foil type gauges, whilst the latter is applicable to any heat transfer gauge made of a material that is thermally dissimilar to that of the surrounding wall.

In the present paper the theory of the convection sensitivity of circular foil gauges is summarised as a basis for the design of the new calibration facility. The experimental design, method and data processing techniques are then presented along with some preliminary experimental results.

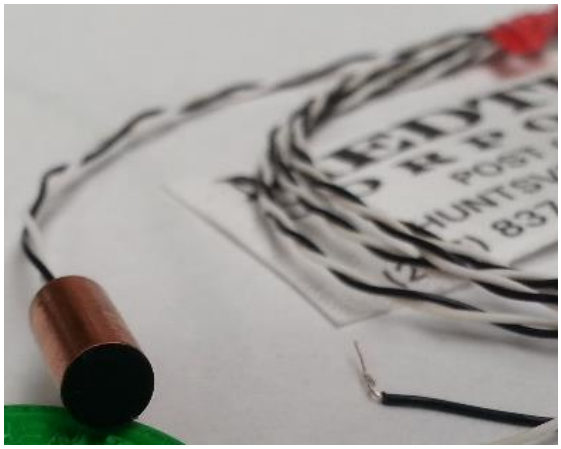

Figure 1: A typical 5mm diameter Gardon Gauge as used in the present study.

A typical Gardon gauge used in the present study is shown in Figure 1, whilst a schematic of a Gardon Gauge is shown in Figure 2. The gauge is constructed of a thin (typically 50 μm) constantan foil welded to a 5 mm diameter cylindrical copper base, with copper wires attached to the centre and edge of the foil (or any point on the base, which is assumed to be isothermal owing to the high thermal conductivity of copper). The construction of the gauge is discussed in more detail by various authors [1, 2, 3, 4].

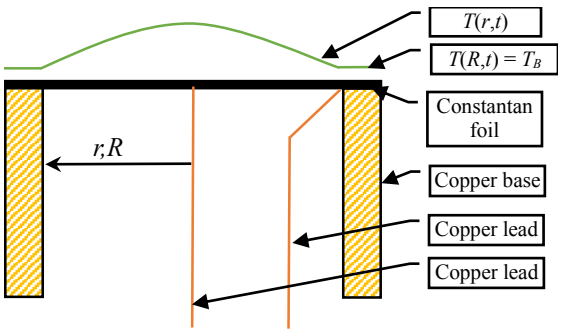

Figure 2: Schematic cross-section of a Gardon Gauge showing arbitrary temperature distribution.

NOMENCLATURE

A^*	Sonic area (at choked orifices) [mm^2]
Bi	Gauge Biot number = $R^2 h_{foil}/\delta k$
d	Nozzle-to-plate distance [mm]
D	Jet nozzle diameter [mm]
h	convective heat transfer coefficient [W/m^2 K]
h_{foil}	Surface-averaged convective heat transfer coefficient on the foil [W/m^2 K]
k	Thermal conductivity [W/m K]
$\dot{m}$	Mass flow [g/s]
Ma	Mach number
NIST	National Institute of Standards and Technology
P_0	Supply total pressure [bar absolute]
q_r	Radiative heat flux to the foil [W/m^2]
q_{foil}	Surface-averaged heat flux incident on the foil [W/m K]
r	Radial coordinate from centre of foil [m]
R	Foil outer radius [m]
Re_D	Reynolds Number based on jet nozzle diameter
t	Time [s]
T	Gauge foil temperature [K]
T_0	= $T(0,t)$ Temperature at the centre of the foil [K]
T_{aw}	Adiabatic wall temperature [K]
T_B	=$T(R,t)$ Gauge copper base temperature [K]
T_{foil}	Surface-averaged foil surface temperature [K]
T_{rad}	Temperature of radiating disc at nozzle inlet [K]
T_i	Substrate initial temperature [K]
T_r	Radiating body temperature [K]
T_s	Substrate surface temperature [K]
T_w	Copper plate wall temperature [K]
α	Thermal diffusivity [m^2/s]
δ	Foil thickness [m]
ε	Emissivity
σ	Stefan-Boltzmann constant [W/m^2 K^4]

GARDON GAUGE THEORY

The foil is assumed to be thin enough such that conduction vertically through the foil is negligible. The one-dimensional heat diffusion equation for the foil may therefore be written:

$$\frac{d^2T}{dr^2}+\frac{1}{r}\frac{dT}{dr}+\frac{h_{foil}}{\delta k}(T_{\mathrm{aw}}-T)+\frac{q_r}{\delta k}=\frac{1}{\alpha}\frac{dT}{dt}, \quad (1)$$

where $T(r,t)$ is the foil temperature. This equation may be solved via judicious substitutions by either separation of variables or Laplace transforms, subject to the boundary conditions $T(r=R,t) = T_B$ (temperature at the foil edge fixed by the base), $\mathrm{d}T(r=0,t)/\mathrm{d}r = 0$ (temperature distribution is symmetrical about the gauge axis), and the initial condition $T(r,t=0) = T_B$ (foil is initially isothermal). Additionally it is assumed that, q_r, the radiative heat flux to the foil, is constant for a radiating body much hotter than the foil. This yields two steady state solutions for the different heat transfer modes:

$$T = T_B + \frac{q_r R^2\left(1-\left(\frac{r}{R}\right)^2\right)}{4\delta k}, \quad (2)$$

for pure radiation (no convection); and

$$T = T_{aw} + (T_B - T_{aw})\left(\frac{I_0\left(\sqrt{\mathrm{Bi}}\frac{r}{R}\right)}{I_0\left(\sqrt{\mathrm{Bi}}\right)}\right), \quad (3)$$

for pure convection (no radiation). For the case of mixed convection and radiation, a third solution may be obtained by substituting T_{aw} in Equation (3) for $T_{aw} + q_r/h_{foil}$, where q_r is the radiative heat flux, assumed constant. These three steady state solutions, as well as their transient counterparts, have been discussed previously by numerous authors [1, 5, 6, 7, 8, 9].

Under steady state conditions, the heat transferred from the foil to the base is equal to the total heat flux incident on the foil surface (by convection and/or radiation). The surface-averaged heat flux to the foil may therefore be written:

$$q_{foil} = \frac{-k2\pi R\delta\left.\frac{dT}{dr}\right|_{r=R}}{\pi R^2} = -\frac{2\delta k}{R}\left.\frac{dT}{dr}\right|_{r=R}. \quad (4)$$

The thermoelectric output of the gauge, which is effectively a T-type thermocouple with its hot junction at the centre of the foil and its cold junction at the copper base, is assumed to be linear over typical temperature ranges encountered in practice, therefore the gauge voltage output is directly proportional to the centre-to-edge temperature difference, $\Delta T=T_0-T_B$ (i.e. $\varepsilon = K_2\Delta T$, where K_2 is the copper-constantan thermoelectric constant). Both the foil-edge temperature differential and the centre-to-edge temperature difference may be evaluated from the above solutions for the temperature distribution in the foil, and equation (4) re-cast as the surface-averaged incident heat flux to the foil, q_{foil}, in terms of the centre-to-edge temperature difference, ΔT. Two expressions may thus be obtained for the surface-averaged gauge incident heat flux in terms of ΔT, as follows:

$$q_{foil} = \frac{4\delta k}{R^2}\Delta T, \quad (5)$$

for pure radiation (no convection) [1]; and

$$q_{foil} = \frac{2\delta k\sqrt{Bi}}{R^2}\left[\frac{I_1\left(\sqrt{Bi}\right)}{I_0\left(\sqrt{Bi}\right)-1}\right]\Delta T, \quad (6)$$

for both pure convection [10, 11] and for mixed convection and radiation [12].

Both of these expressions may be inverted and ΔT substituted for ε / K_2 in order to obtain the voltage sensitivity to incident heat flux. It is apparent from these two expressions that the gauge sensitivities with and without convection are very different. Equation (5) represents the linear calibration that is typically done by the manufacturer in a radiation oven. Equation (6) represents the correct calibration if the gauge is used in convective environments, hence there is a need to develop a straightforward calibration method for the end-user.

Dividing (6) by (5) yields the ratio of mixed heat flux incident on the gauge foil to that obtained using just the factory calibration:

$$\frac{q_{foil}}{q_{raw}} = \frac{\sqrt{Bi}}{2}\left[\frac{I_1\left(\sqrt{Bi}\right)}{I_0\left(\sqrt{Bi}\right) - 1}\right]. \qquad (7)$$

This equation allows the raw heat flux to be corrected to give the heat flux incident on the foil, however, this is *not* the same as the undisturbed heat flux to the surrounding wall. This may be described by:

$$q_{wall} = q_r + h_{wall}(T_{aw} - T_{wall}), \qquad (8)$$

whilst the heat flux to the gauge foil is described by:

$$q_{foil} = q_r + h_{foil}\left(T_{aw} - T_{foil}\right). \qquad (9)$$

It is apparent that the surface-averaged heat flux to the foil is not the same as that to the undisturbed wall since the surface-averaged foil temperature is not equal to the wall temperature owing to the temperature distribution in the foil. Assuming perfect thermal contact between the base and the wall so that T_{wall} is equal to T_B, Equation (8) may be substituted into the theoretical expression for ΔT in equation (6), and this expression rearranged to yield the ratio between the foil and undisturbed wall heat flux:

$$\frac{q_{foil}}{q_{wall}} = \frac{2}{\sqrt{Bi}}\frac{I_1\left(\sqrt{Bi}\right)}{I_0\left(\sqrt{Bi}\right)}. \qquad (10)$$

This expression also assumes that $h_{foil} = h_{wall}$. Equation (10) may be combined with Equation (7) to obtain the ratio of true undisturbed wall heat flux to that obtained using just the factory calibration [12]:

$$\frac{q_{wall}}{q_{raw}} = \frac{Bi}{4}\left[\frac{I_0\left(\sqrt{Bi}\right)}{I_0\left(\sqrt{Bi}\right) - 1}\right]. \qquad (11)$$

Thus for a Gardon gauge that comes factory calibrated for radiation according to Equation (5) it is necessary to determine the calibration correction in Equation (11) if this gauge is to be used in convective environments. Where possible the gauge should be calibrated for a range of heat transfer coefficients as close as possible to those encountered in the measurement application.

EXPERIMENTAL FACILITY

The transient convection calibration facility designed and built at the Osney Thermo-Fluids Laboratory is a development of an earlier transient facility used for determining the thermal product of thin film gauge substrates, the "Shutter Rig", developed by Piccini et al. [13]. As well as calibrating Gardon gauges, the new facility was designed to be able to calibrate other heat transfer gauges and probes in both cross-flow (flat plate) and impingement configurations over a range of heat transfer coefficients and gas temperatures in a low-turbulence flow.

The advantage of the transient technique employed here over the steady state calibration facilities developed previously [11, 14, 15, 16] is that it does not require water cooling, thus simplifying the experimental design as well as costs, and the measurement location does not need to reach steady state, thus permitting reduced experimental run-time.

The new transient convection calibration facility is shown in Figure 3. The facility is connected to a 100psi air supply. A system of choked orifices is used together with an upstream regulator to fix the mass flow through the facility. The orifice fittings themselves have interchangeable throat sections, and may be used in parallel, thus allowing a range of fixed and repeatable flow conditions. The air then passes through a 42 kW 3-phase heater, capable of heating it to 500 °C. This particular heater was selected for its relatively low cost and large flow area thus permitting a wide range of nozzle contraction ratios and flow configurations (the heater can also be connected to a square duct so that rectangular cross-section "letterbox" nozzles can be attached for flat plate tests). For the present tests the nozzle attached to the exit of the heater had a 26 mm diameter circular exit and a contraction ratio of approximately 6:1. The nozzle exit area is large in comparison to the gauge diameter (5 mm) ensuring a uniform flow over the surface of the gauge.

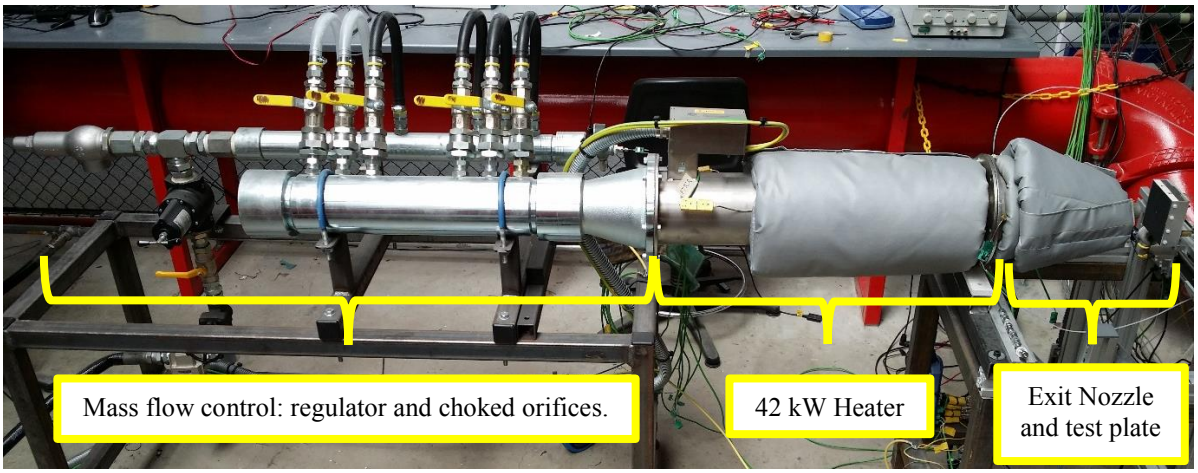

Figure 3: The new transient convection calibration experimental facility.

The nozzle exit area is large in comparison to the gauge diameter (5 mm) ensuring a uniform flow over the surface of the gauge.

Heat transfer gauges are attached to plates at the nozzle exit, themselves mounted on a fast-traverse mechanism. The fast-traverse mechanism is actuated by a pair of elasticated 'bungee' cords that can be quickly hooked and unhooked, and which, unlike motorised traverse mechanisms, benefit from zero electrical noise. The tension in the bungee cords, hence traverse time, is adjustable by adjusting the stretched length as well as the cord thickness (by swapping the cords). The plates are mounted on carriages that connect to the bungee cords. Overall the traverse time is only a few tenths of a second, and the motion is highly repeatable. The traverse also allows the plate height and nozzle-to-plate spacing to be adjusted, therefore the impingement heat transfer coefficient can be adjusted by the nozzle-to-plate spacing as well as the choked orifice selection. The traverse can also be converted to a "flat-plate" shear flow configuration if required.

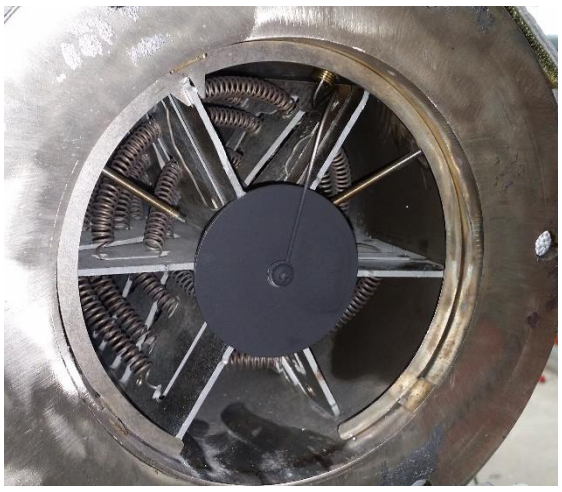

Figure 4: The radiation measurement device.

In order to determine the radiation heat flux at the nozzle exit due to the heater elements, a 50 mm diameter metal disc was placed downstream of the elements at the heater exit and a thermocouple affixed to measure the disc temperature (Figure 4). The disc was painted black with a standard high-temperature high-emissivity automotive exhaust paint manufactured by James Briggs Ltd, Oldham, UK, OL2 6HZ.

A dual thermocouple-pitot probe was located downstream of the nozzle exit flow in order to obtain the approximate total flow conditions at the gauge location. The probe was positioned so that the sensing elements (the thermocouple bead and Pitot tube inlet) were located at the same location as the heat transfer gauges once the plates were at rest in the flow. The probe features a tail fin to maintain its position in the flow, and was designed to rotate so that on traversing the flow the plates cause the probe to rotate out of the flow without damaging the probe.

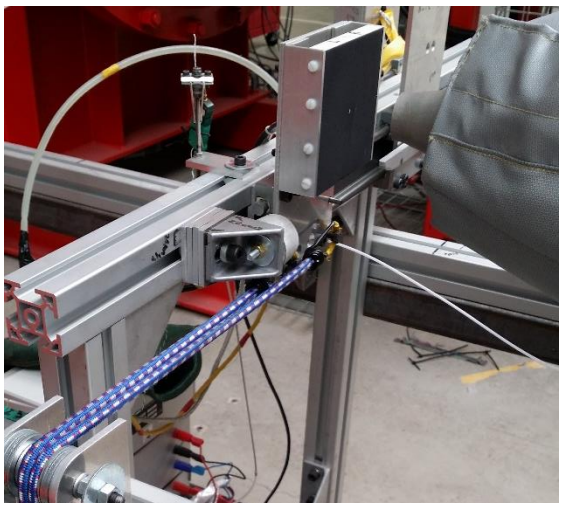

Figure 5: The spring-loaded traverse, with MACOR plate in position and pitot/thermocouple probe rotated out of the flow.

Two thermocouples were also placed at the nozzle inlet, along with a Pitot tube and static tapping, in order to measure the nozzle inlet conditions. Two further thermocouples were built in to the heater exit to monitor the heater exit temperature.

EXPERIMENTAL METHOD

The method used to calibrate the Gardon gauge involves the use of two geometrically identical square plates, one made from Corning MACOR® machineable glass ceramic, the other from Copper. Both plates are mounted in the fast-traverse carriage in a vertical impingement configuration so that the centre of each plate aligns with the nozzle axis once the plate comes to rest after being traversed into the flow. The plates are traversed into the flow one after the other in quick succession to ensure identical flow conditions for each traverse. The time taken to swap the plates is about 2 to 3 minutes.

Figure 6: The MACOR impingement plate before painting with high-emissivity high-temperature paint.

The MACOR plate features a 1x2mm hand-painted platinum thin-film gauge (Figure 6) located at the centre, whilst the copper plate features the Gardon gauge, mounted at the same location (Figure 8). Both plates are 100mm square by 13mm thick, and both plates also feature a series of thermocouples on the front and back surfaces to ensure each plate is isothermal before the start of a run. Both plates are also painted with high-emissivity high-temperature exhaust paint (the same as that used to paint the radiation measurement device) in order to allow the surface temperature to be measured using an infra-red camera. The plates are shown before painting in Figure 6 and Figure 8, so that the instrumentation is visible, whilst the MACOR plate is shown after painting in Figure 5. The plates were painted simultaneously to ensure an identical surface finish. The voltage signals from the heat transfer sensors on both plates are amplified before being recorded on a PC-based data acquisition system sampling at 50 Hz. The thermocouple signals are also recorded on the same PC at a sampling rate of 1 Hz.

The geometry and thermal properties of the MACOR plate mean that the heat conduction within the plate remains one-dimensional and semi-infinite for around 15 seconds from the start of each run. The impulse response method [17] is used to determine the heat flux from the surface temperature history, and the heat flux is then plotted versus surface temperature in q-T space, and Equation (12) is fitted to the data in order to obtain both the adiabatic wall temperature and the heat transfer coefficient. Note that this equation is a fourth order polynomial that accounts for both convection and radiation, as opposed to the straight line that is normally used to fit q-T data when radiation is negligible. The radiation heat flux in Equation (12) is obtained from the temperature measurement at the nozzle inlet as previously discussed. The temperature and heat flux histories are first smoothed in time using a hamming window around 5% of the length of the data in points, and then the signals cropped to remove transient end-effects due to the filtering. An example of the polynomial fit, alongside the raw data and smoothed and cropped data, is shown in Figure 7.

$$q = h_{wall}(T_{aw} - T_{wall}) + \varepsilon\sigma\left({T_r}^4 - {T_{wall}}^4\right) \quad (12)$$

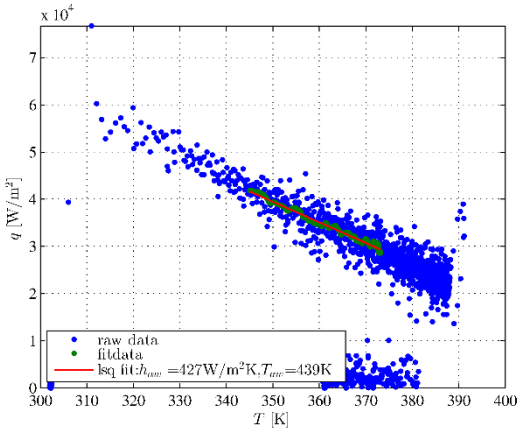

Figure 7: The polynomial fit to obtain h_{wall} and T_{aw}

The MACOR plate thin film surface temperature measurements are also used to calibrate the infra-red camera that is subsequently used to measure the copper plate surface temperature. This in-situ calibration takes into account the paint properties and the effects of viewing angle, both of which are identical between the two plates. The transient calibration was checked against a steady-state oven calibration and the results were found to be in excellent agreement.

Once the MACOR plate has been traversed, the plate-carriage assembly is removed from the flow and quickly swapped for the carriage containing the copper plate (Figure 8). The copper plate is then traversed to the same position in the same flow. The surface temperature of the copper plate is measured using the IR camera and the average surface temperature in a thin ring around the Gardon gauge base is computed. This surface temperature along with h and T_{aw} found using the MACOR plate allow the undisturbed wall heat flux to be obtained. The raw uncorrected heat flux is found from the Gardon gauge voltage signal using the factory calibration, from which the radiation heat flux is then subtracted to isolate the purely convective heat flux. Thus the average ratio of the two heat fluxes can be found.

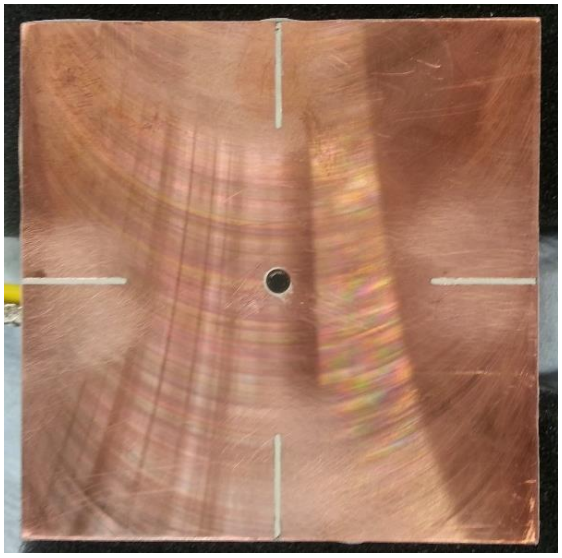

Figure 8: The copper impingement plate before painting with high-emissivity high-temperature paint.

An example of the uncorrected raw Gardon gauge heat fluxes, before and after subtraction of the radiative heat flux (also shown), and the undisturbed wall convective heat flux, is shown in Figure 9.

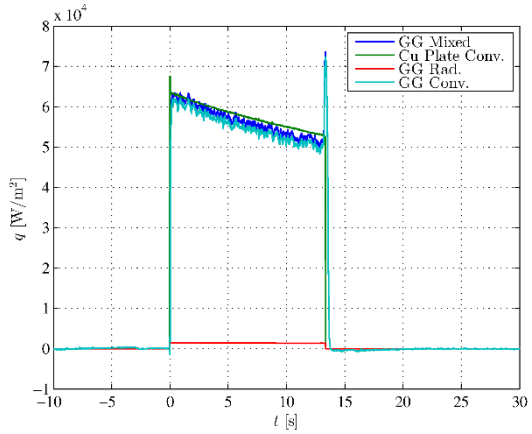

Figure 9: Copper plate heat fluxes for a typical run.

This procedure was repeated for the flow conditions given in Table 1 by varying the inlet orifice combination whilst the heater input power was adjusted to maintain the same gas temperature for all runs. Experimental data is thus obtained for the correction ratio as a function of h_{foil}, and Equation (11) is then fitted to this data, by varying the parameter $R^2/\delta\, k$. Thus the correction ratio for the given gauge may be extrapolated for any given heat transfer coefficient.

P_0 [bar]	A^* [mm^2]	$\dot{m}$ [g/s]	U_{jet} [m/s]	Ma	Re$_D$	T_{rad} [K]
4.24	79	48	128	0.37	211593	417
4.15	201	120	186	0.55	332788	425
3.82	280	154	248	0.75	488786	445
2.88	434	181	-	-	-	438

Table 1: Flow conditions for the four tests conditions presented. Nozzle diameter D was 26mm, and nozzle-to-plate spacing d was 28mm, for all tests. Velocity could not be obtained for the final test point as the pitot probe failed.

INITIAL RESULTS AND DISCUSSION

The results from an initial Gardon gauge calibration at approximately 120 °C gas temperature for heat transfer coefficients between 275 and 475 W/m^{2}K are shown in Figure 10. The red line is the theoretical curve based on Equation (11) with the manufacturer's quoted values for R, and δ, and a standard value for k for constantan. The green curve is the best fit of Equation (11) to the experimental data. Whilst a full uncertainty analysis is still to be conducted, there is approximately +/- 3% variance around the line of best fit to the present data, and it is likely that overall experimental uncertainty will be of similar order. For comparison, previous steady state studies over several years at NIST have quoted uncertainties between +/- 10% [18] and +/- 3% [14], the latter figure being obtained using a second iteration of the original facility that produced the former. Heat flux is notoriously difficult to measure with accuracy better than +/- 10%, and +/- 5% uncertainty is typical for such measurements (e.g. [16]).

These results demonstrate the difference between the manufacturer-specified and actual sensitivity in convective environments, and thus the importance of performing the calibration. Future tests will focus on tracing and reducing sources of uncertainty, as well as investigating the effects of gas temperature and stream-wise wall-temperature profile effects in flat plate (shear flow) configuration.

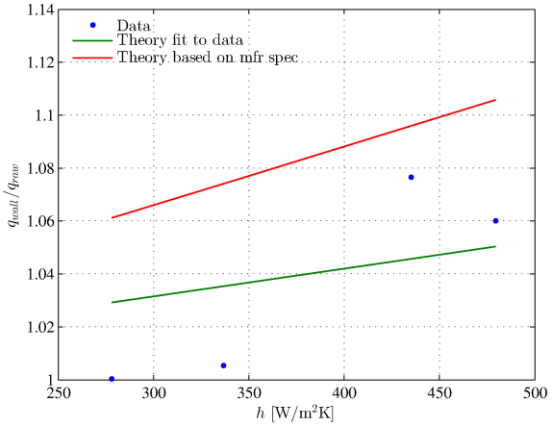

Figure 10: The initial convection calibration correction.

CONCLUSIONS

A novel transient method for calibrating heat transfer gauges for convection measurements in high enthalpy flows has been demonstrated. The new method does not require water cooling to induce heat transfer, thus the experimental facility is simple, inexpensive, easy to adapt for different flow configurations and quick to run across a wide range of flow conditions. Any laboratory intending to make convective heat flux measurements in turbomachines and other high temperature environments should consider the transient calibration method as a simple, versatile and cost-effective alternative to steady state methods.

ACKNOWLEDGMENTS

This work was supported by Mitsubishi Heavy Industries - Takasago Research & Development Centre, Takasago, Hyogo, 676-8686, Japan.

The authors acknowledge the work and skill of Trevor Godfrey, Dominic Harris and Gerald Walker at the Osney Thermo-Fluids Laboratory in constructing and instrumenting the new facility.

REFERENCES

[1] Gardon, R. , 1953, "An instrument for the direct measurement of intense thermal radiation," *Rev. Sci. Instrum.*, vol. 24, no. 5, pp. 366-370.

[2] Stempel, F. C., 1966, "Metallurgically Bonded Circular Foil Heating Rate Sensor," US Patent 3,280,626.

[3] Trimmer, L. L., Matthews, R. K., and Buchanan, T. D., 1973, "Measurement of Aerodynamic Heat Rates at the von Kármán Facility," in *ICIASF '73 Record: International Congress on Instrumentation in Aerospace Simulation Facilities*, Calif. Institute of Technology, 10-12 September, pp. 35-44, IEEE Aerospace and Electronic Systems Society, New York.

[4] Lee, Y. H., Koo, S. W., and Choi, J. H., 2005, "Heat-flux gage, manufacturing method and manufacturing device thereof," US Patent 6,837,614.

[5] Malone, E. W., 1968, "Design and Calibration of Thin-Foil Heat Flux Sensors," *ISA Transactions*, vol. 7, no. 3, pp. 175-180.

[6] Ash, R. L., 1969, "Response Characteristics of Thin-Foil Heat Flux Sensors," *AIAA Journal*, vol. 7, no. 12, pp. 2332-2335.

[7] Kirchhoff, R. H., 1972, "Response of Finite-Thickness Gardon Heat Flux Sensors," *J. Heat Transfer*, vol. 94, no. 2, pp. 244-245.

[8] Keltner, N. R. and Wildin, M. W., 1975, "Transient response of circular foil heat-flux gauges to radiative fluxes," *Rev. Sci. Instrum.*, vol. 48, no. 9, pp. 1161-1166.

[9] Grothus, M. A., Mulholland, G. P., Hills, R. G., and Marshall, B. W., 1983, "The transient Response of Circular Foil Heat Flux Gages," Report SAND83-0263, Sandia National Laboratories, Albuquerque, NM.,.

[10] Prasad, B. V. and Mohanty, A. K., 1983, "Analysis and calibration of a foil heat flux sensor for convective measurements," *J. Phys. E: Sci. Instrum.*, vol. 16, no. 11, pp. 1095-1099.

[11] Borell, G. J. and Diller, T. E., 1987, "A Convection Calibration Method for Local Heat Flux Gages," *J. Heat Transfer*, vol. 109, no. 1, pp. 83-89.

[12] Kuo, C. H. and Kulkarni, A. K., 1991, "Analysis of Heat Flux Measurement by Circular Foil Gages in a Mixed Convection/Radiation Environment," *J. Heat Transfer*, vol. 113, no. 4, pp. 1037-1040.

[13] Piccini, , E. , Guo, S. M., and Jones, T. V., 2005, "The development of a new direct-heat-flux gauge for heat-transfer facilities," *Meas. Sci. Technol.*, vol. 11, no. 4, pp. 342-349.

[14] Holmberg, D. , Womeldorf, C. , and Grosshandler, W. , 1997, "Design and uncertainty analysis of a second-generation convective heat flux calibration facility," in *HTD-Vol 364-4, Proceedings of the ASME Heat Transfer Division*, vol. 4, pp. 65-70.

[15] Gifford, A. , Hoffie, A. , Diller, T. , and Huxtable, S. , 2010, "Convection Calibration of Schmidt-Boelter Heat Flux Gauges in Stagnation and Shear Air Flow," *J. Heat Transfer*, vol. 132, no. 3, pp. 031601-1-031601-9.

[16] Stathopoulos, P. , Hofman, F. , Rothenfluh, T. , and von Rohr, P. R., 2012, "Calibration of a Gardon Sensor in a High-Temperature High Heat Flux Stagnation Facility," *Experimental Heat Transfer*, vol. 25, no. 3, pp. 222-237.

[17] Oldfield, M. L., 2008, "Impulse Response Processing of Transient Heat Transfer Gauge Signals," *J. Turbomach.*, vol. 130, no. 2, pp. 021023-1-021023-9.

[18] Holmberg, D. , Steckler, K. , Womeldorf, C. , and Grosshandler, W. , 1997, "Facility for calibrating heat flux sensors in a convective environment," in *HTD-Vol 353, Proceedings of the ASME Heat Transfer Division*, vol. 3, pp. 165-171.